

# Commensurate and Incommensurate Lattice Distortions in DySe<sub>1.85</sub> and Rb<sub>0.33</sub>DySe<sub>2.67</sub>

Brendan Foran,<sup>†</sup> Stephen Lee,<sup>\*†</sup> and Meigan C. Aronson<sup>‡</sup>

Willard H. Dow Chemistry and Randall Physics Laboratories, University of Michigan, Ann Arbor, Michigan 48109-1055

Received February 2, 1993. Revised Manuscript Received April 19, 1993

We report the synthesis and structure of two new compounds, DySe<sub>1.84</sub> and Rb<sub>0.33</sub>DySe<sub>2.67</sub>. Both structures are new structural variants of the Cu<sub>2</sub>Sb and NdTe<sub>3</sub> structure types. DySe<sub>1.84</sub> has an incommensurate lattice distortion, and Rb<sub>0.33</sub>DySe<sub>2.67</sub> contains a site occupancy wave. The substructure of DySe<sub>1.84</sub> is tetragonal with *P4/nmm* symmetry with *a* = 4.0124(5) Å and *c* = 8.261(2) Å with final *R/R<sub>w</sub>* = 2.0/1.8%. The substructure of Rb<sub>0.33</sub>DySe<sub>2.67</sub> is orthorhombic with space group *Cmcm* and *a* = 4.0579(6) Å, *b* = 26.47(1) Å and *c* = 3.8909(6) Å with final *R/R<sub>w</sub>* = 3.7/1.9%. In both structures there is a clear shift of Se atoms away from high symmetry positions. We also report extended Hückel band calculations which suggest the incommensurate superlattice found in DySe<sub>1.84</sub> is of charge density wave type.

## Introduction

Transition-metal chalcogenides have played an important role in solid-state and materials chemistry for a number of years. Much of the interest in these materials stems from the discovery of charge density waves in compounds such as NbSe<sub>3</sub>, Ta<sub>1-x</sub>Ti<sub>x</sub>S<sub>2</sub> and TaTe<sub>2</sub>, of site occupancy waves in chromium sulfides or selenides, of superconductivity in Chevrel phases, and of intercalation chemistry in early transition metal dichalcogenides such as TiS<sub>2</sub> and TiSe<sub>2</sub>.<sup>1</sup> Many of these properties can be directly related to the low dimensionality of these materials.

Comparatively little effort has been directed to the rare-earth analogs of the transition-metal chalcogenides. This is of interest as one can establish a formal analogy between transition-metal dichalcogenides such as TaSe<sub>2</sub> or NbSe<sub>2</sub> and rare earth compounds such as DySe<sub>2</sub>. In the former compounds there is nominally one electron in an otherwise empty d-band. This single d-electron coupled with the two-dimensional character of the material is the driving force behind the charge density waves (CDW) observed in these materials.<sup>2</sup> By contrast, DySe<sub>2</sub> has one hole in the otherwise filled Se p-band. Furthermore DySe<sub>2</sub>, like TaSe<sub>2</sub> and NbSe<sub>2</sub>, also forms in an anisotropic two-

dimensional sheet structure.<sup>3</sup> However to our knowledge, there has been no study of incommensurate CDW formation in rare earth dichalcogenides such as DySe<sub>2</sub>.<sup>4</sup>

In this paper we report the synthesis and structure of DySe<sub>1.84</sub> and Rb<sub>0.33</sub>DySe<sub>2.67</sub> (RbDy<sub>3</sub>Se<sub>8</sub>). The former material has an incommensurate superstructure which we tentatively assign to be of CDW type. The latter compound contains site occupancy waves (SOW) analogous to SOW's found in Ti<sub>1+x</sub>S<sub>2</sub>, Cr<sub>1+x</sub>S<sub>2</sub>, Cr<sub>1+x</sub>Se<sub>2</sub>, K<sub>5</sub>Se<sub>3</sub>, and M<sub>x</sub>K<sub>4</sub>Te<sub>3</sub> (M = Ca, Sr).<sup>1g-1</sup> Finally it is found that the Rb atoms in the former material lie in positions highly reminiscent of alkali metal positions in intercalated transition metal dichalcogenides.<sup>1m,n</sup> The studies reported here complement earlier work by Urland and Plambeck-Fischer and others who have found SOW and commensurate CDWs in LaSe<sub>1.9</sub>, PrSe<sub>1.9</sub> and CeSe<sub>1.9</sub> and Benazeth, Marcon, and others have found commensurate CDWs (i.e., formation of Se<sub>2</sub><sup>2-</sup> dimers) in LaSe<sub>2</sub>.<sup>5</sup>

## Experimental Section

All samples were prepared from mixtures of Dy, Se, RbCl, and LiCl. Nominal purities were Dy 99.9% (40 mesh), Se 99.999%, RbCl 99.8%, and LiCl 99+% pure, all from Aldrich. The LiCl and RbCl were melted under flame and left for several minutes under a 10<sup>-3</sup>-Torr vacuum. We placed approximate 1-g samples of one part Dy to two parts Se together with 2 g of LiCl/RbCl (LiCl varying between 45-55 atm % of the halide mixture) in sealed quartz tubing. The LiCl/RbCl fluxes melt between 300 and 450 °C.<sup>6</sup> We heated the combined samples to 680 °C over

<sup>†</sup> Dow Laboratory.

<sup>‡</sup> Randall Laboratory.

(1) (a) CDW formation: Wilson, J. A.; DiSalvo, F. J.; Mahajan, S. *Adv. Phys.* 1975, 24, 117. (b) Rouxel, J., Ed. *Crystal Chemistry and Properties of Materials with Quasi-One-Dimensional Structures*; Reidel: Dordrecht, Holland, 1986. (c) Monceau, P.; Ong, N. P.; Portis, A. M.; Meerschaut, A.; Rouxel, J. *Phys. Rev. Lett.* 1976, 10, 602. (d) Chevrel phases: Chevrel, R.; Sergent, M.; Prigent, J. *J. Solid State Chem.* 1971, 3, 515-519. For reviews, see: (e) Fisher, Ø. *Appl. Phys.* 1978, 16, 1-28. (f) Chevrel, R. In *Superconductor Materials Science: Metallurgy, Fabrication and Applications*; Foner, S., Schwartz, B. B., Eds.; Plenum Press: New York, 1981; Chapter 10. (g) Site occupancy waves: Titanium sulfide: Wieggers, G. A.; Jellinek, F. *J. Solid State Chem.* 1970, 1, 519. (h) Chromium sulfides: Jellinek, F. *Acta Crystallogr.* 1957, 10, 620. (i) Chromium selenides: Wehmeier, F. H.; Keve, E. T.; Abrahams, S. C. *Inorg. Chem.* 1970, 9, 2125. (j) K<sub>5</sub>Se<sub>3</sub>, Cs<sub>5</sub>Te<sub>3</sub>, and Cs<sub>2</sub>Te: Schewe-Miller, I.; Böttcher, P. *Z. Kristallogr.* 1991, 196, 137. (k) M<sub>x</sub>K<sub>4</sub>Te<sub>3</sub> (M = Ca, Sr): Schewe-Miller, I.; Böttcher, P. *J. Alloys Compn.* 1992, 183, 98. (l) Nb-Ta-S phases: Yao, X.; Franzen, H. F. *Z. Anorg. Allg. Chem.* 1991, 598/599, 353. (m) Intercalation: Whittingham, M. S.; Jacobson, A. J. *Intercalation Chemistry*; Academic: New York, 1982. (n) Rouxel, J. *Physica* 1980, 99B, 3.

(2) Whangbo, M. H.; Canadell, E. *J. Am. Chem. Soc.* 1992, 114, 9587.

(3) (a) NbTe<sub>2</sub> and TaTe<sub>2</sub>: Brown, B. E. *Acta Crystallogr.* 1966, 20, 264. (b) TaSe<sub>2</sub>: Brouwer, R.; Jellinek, F. *Physica* 1980, 99B, 51. (c) Rare-earth diselenides: Haase, D. J.; Steinfink, H.; Weiss, E. *J. Inorg. Chem.* 1965, 4, 538. (d) Wang, R.; Steinfink H. *Inorg. Chem.* 1967, 60, 1685.

(4) A preliminary report of an incommensurate structure is however reported for PrSe<sub>2.0</sub> in: Plambeck-Fischer, P.; Urland, W.; Abriel, W. *Z. Kristallogr.* 1987, 178, 182. However these authors do not report the actual incommensurate lattice vector in their preliminary report.

(5) (a) Se<sub>2</sub><sup>2-</sup> formation in CeSe<sub>2</sub>: Marcon, J.-P.; Pascard, R. *C.R. Acad. Sc. Paris* 1968, 266, 270. (b) Se<sub>2</sub><sup>2-</sup> formation in LaSe<sub>2</sub>: Bénazeth, S.; Carré, D.; Laruelle, P. *Acta Crystallogr.* 1982, B38, 33 (c) LaSe<sub>2-x</sub> superstructures: Benazeth, S.; Carré, D.; Guittard, M.; Flahaut, J. C. *R. Acad. Sc. Paris* 1975, 280, 1021. (d) LaSe<sub>1.9</sub>: Grupe, M. Urland, W. *J. Less. Comm. Met.* 1991, 170, 271. (e) CeSe<sub>1.9</sub> and PrSe<sub>1.9</sub>: Plambeck-Fischer, P.; Abriel, W.; Urland, W., *J. Solid State Chem.* 1989, 78, 164. (6) Zhemchuzhnyi, S.; Rambach, F. *Z. Anorg. Allg. Chem.* 1910, 65, 408.

the course of 1 week and then cooled to 450 °C at the rate of 0.04 °C/min. At this point the furnace was turned off, and the samples were cooled to room temperature while still in the furnace. The quartz tubes were broken and the product was washed with water, ethanol, and acetone to remove first the salt and then the water. Samples were then stored under an inert atmosphere. Powder X-ray photographs were taken of the products (Enraf-Nonius Guinier camera,  $Cu K\alpha_1$  radiation, and NBS Si internal standard). We analyzed single crystals by electron microprobe (Cameca MBX automated microprobe, WDS for quantitative stoichiometry and KEVEX EDS for nonstandardized measurements). Samples were analyzed for Dy, Se, Si, O, Rb, and Cl. Li analysis was done on bulk material by Galbraith. Standards for WDS were  $Dy_2Ga_5O_{12}$  for Dy and elemental selenium for Se. Rotation, Weissenberg ( $Cu K\alpha$  radiation) and precession ( $Mo K\alpha$  radiation) photographs were taken to select crystals for X-ray diffraction data collection, to determine crystal class, and to search for weak superstructure reflections. We found such film methods were essential in the determination of the superstructure cells of the reported compounds. The conditions for the four-circle diffraction data collections are given in the supplementary material (see paragraph at end of paper).

## Results

The principal product of the reaction was in the form of greenish-gold platelets. Microprobe analysis of these platelets gave a stoichiometry of  $Rb_{0.09(2)}Dy_{0.23(2)}Se_{0.68(4)}$ . No Si, O, or Cl was observed in the microprobe analysis of this phase. Chemical analysis for a bulk sample (Galbraith) gave a Li content of 0.85 mol %. However, we cannot rule out the possibility that the Li atoms belong to an impurity phase which is at too low a concentration to be observed by X-ray powder analysis. The microprobe stoichiometry was corroborated by the final single-crystal structure refinement which led to a final stoichiometry of  $Rb_{0.08Dy_{0.25}Se_{0.67}}$ . The powder diffraction pattern for this phase could be indexed with an orthorhombic unit cell of  $a_{sub} = 4.0580(6)$  Å,  $b_{sub} = 26.47(1)$  Å,  $c_{sub} = 3.8909(6)$  Å. Powder diffraction lines obeyed a C-centering law, i.e.,  $h + k$  = even for  $hkl$  reflections. Weissenberg and rotation photographs indicated a very weak superstructure with  $a_{super} = 4a_{sub}$ ,  $b_{super} = b_{sub}$ , and  $c_{super} = 3c_{sub}$ . Heretofore, we have been unable to find a large enough single crystal to record accurate intensities for superstructure reflections. For example, on the crystal chosen for single-crystal X-ray data collection, the most intense superstructure reflections were  $10^{-3}$  the intensity of the principal substructure reflections. We therefore report here only the substructure of this phase.

In addition, a well-crystallized minor product was found in our reaction mixture. This product appeared as small copper platelets. Microprobe analysis gave a stoichiometry of  $DySe_{1.87(2)}$ . No traces of Si, O, Rb, or Cl were observed in the microprobe analysis of this second phase. We were unable to collect a sufficient amount of sample to measure the trace Li content. The stoichiometry from our microprobe studies are corroborated by the final single-crystal X-ray refinement which gave a stoichiometry of  $DySe_{1.84}$ . The powder pattern of the bulk material contained no additional lines beyond those of the two products reported above.

**X-ray Structure Refinement.**  $DySe_{1.84}$ : A data set was collected on the tetragonal cell previously observed by film methods. Observed diffraction symmetry and systematic absences ( $hk0$ :  $h + k = 2n + 1$  absent) were compatible with the  $P4/nmm$   $Cu_2Sb$  structure reported for  $DySe_2$ .<sup>3c,d</sup> Isotropic refinement of a  $Cu_2Sb$  type trial solution gave reasonable parameters for dysprosium and

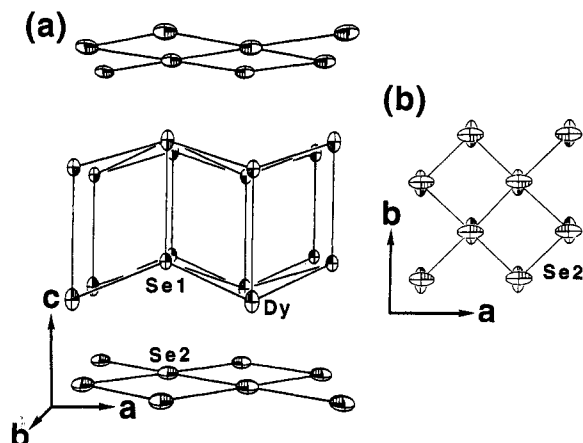


**Figure 1.** (a)  $DySe_{1.84}$  subcell. (b) Single sheet of Se(2). In (a) for the sake of clarity, the Se(2) atoms are drawn as flattened thermal ellipsoids, in (b) we show the reported thermal ellipsoids.

selenium atoms in distorted NaCl layers (Dy and Se(1) in Figure 1), but anomalously large thermal parameters were found for selenium atoms in the square sheets (Se(2)).  $R_w$  was minimized with a 70% occupation of the site corresponding to these problem selenium atoms, but the isotropic thermal parameter was still quite large. Further anisotropic refinement led to an  $R_w = 2.15\%$  for 173 unique reflections and 11 parameters with the partial occupation of the site now 81.5%. Finally, letting occupation factors vary on all sites did not lead to any change in occupation factors by greater than 1.5%.

The final stages of refinement had a number of interesting features to them. Both Dy and Se(1) had thermal ellipsoids which were elongated along the c axis. By contrast Se(2) had a pancake-shaped thermal ellipsoid, flat in the direction of the c axis. As some ellipsoids were elongated while others were flattened, we conclude that absorption correction errors were not responsible for the anomalous thermal factors. Our results parallel an earlier study by us for  $Ta_{1-x}Ti_xTe_2$  crystals where we showed that similarly flattened thermal ellipsoids corresponded to a shift in Ta's atomic position away from a center of symmetry.<sup>7</sup> Here we tested several distortions for the Se(2) atom away from the high symmetry 2(a) site. Distortion in either the a or b direction was preferred over that in the a + b direction (Figure 1b).<sup>8</sup> The final occupation found for this Se(2) site is at 84%. Such proposed distortions might be expected to order and create superlattice diffraction allowing the true solution of the distorted structure. X-ray photographs did show additional superlattice reflections; however, these were not readily indexable as simple multiples of the recorded substructure reflections. Precession and Weissenberg photographs on two separate crystals gave identical superstructure reflection patterns with all superstructure reflections lying at  $\pm 0.276a^* \pm 0.333b^* + 0.5c^*$  from substructure reflections. It is possible that these are satellite peaks resulting from a charge density wave state at lower temperatures (low temperature analyses have not yet been performed). On Weissenberg photos, these superstructure reflections generally appear clearly at high  $\theta$  values.

$Rb_{0.33}DySe_{2.67}$ : As stated earlier, we report here only the structure of the C-centered subcell. The observed systematic extinctions were compatible only with  $Cmc2_1$ ,  $C2cm$ , and  $Cmcm$ . We solved the structure in  $Cmcm$ . This

(7) Lee, S.; Hoistad, L. M.; Kampf, J. *New J. Chem.* 1992, 16, 657.

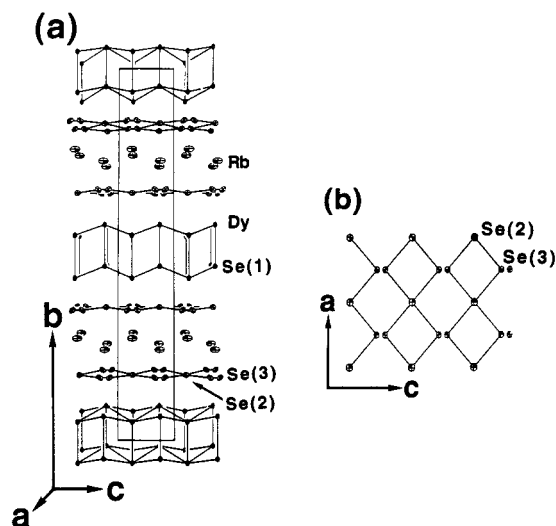


Figure 2. (a)  $\text{Rb}_{0.33}\text{DySe}_{2.67}$  structure. (b) Sheet of Se(2) and Se(3) atoms.

space group and cell dimensions are similar to the  $\text{NdTe}_3$  structure type previously observed for rare earth tritellurides.<sup>10</sup> We therefore chose this structure as the starting point for our refinement. Upon refinement we added an additional atomic position, the Rb atom, to our refinement. Both the Rb atom and the Se(3) atom had anomalously large thermal parameters indicative of only partial occupancy. Therefore, we allowed their site occupancy factors to refine. We found furthermore that the Se(3) atoms left the original site of higher symmetry in the manner illustrated in Figure 2. The final  $R/R_w$  equaled 3.68/1.92% for 26 parameters and 557 unique reflections with occupation factors of 32.4(4)% and 32.8(2)% for respectively

(8) The  $\text{Cu}_2\text{Sb}$  structure in  $P4/nmm$  symmetry accounts for the selenium atoms in the flat square sheets by one symmetry equivalent site; 2(a) at  $(\frac{1}{4}, \frac{3}{4}, 0)$ . Under isotropic refinement,  $R_w$  was minimized to 8.36% with a 70% occupation and  $U_{\text{iso}} = 0.0489$  for this site (the other atoms in the structure had fully occupied sites with normal thermal factors). With anisotropic refinement the thermal ellipsoids of this 2(a) site flattened drastically,  $U_{33} = 0.0093$ , but  $U_{11} = U_{22} = 0.0658$ , giving  $R_w = 2.15\%$  with a site occupation of 80.8% (this is the solution shown in Figure 1a). These flattened ellipsoids led us to consider shifting the atomic sites away from the 4-fold axis within the  $a$ - $b$  plane. We consider two possible Se(2) distortions, that of 8(g) and 8(i) (referring to multiplicity and Wyckoff letter). Under both isotropic and anisotropic refinement the 8(i) site gave (in a statistically significant manner) lower  $R_w$  factors. For isotropic refinement of Se(2), keeping the other atoms anisotropic, the 8(g) solution gave an  $R_w = 3.10\%$  while the 8(i) gave  $R_w = 2.69\%$ . Under anisotropic refinement of all atoms the 8(g) solution gave  $R_w = 2.11\%$  while the 8(i) solution had an  $R_w = 1.66\%$ . Both refinements had an equal number of refined parameters. The final solution for the atomic position Se(2) in the 1.66% refinement is  $(0.285(3), \frac{3}{4}, 0.002(3))$ . In the anisotropic refinement the thermal ellipsoids for the 8(i) sites resembled perpendicular cigars lying in the  $a$ - $b$  plane, intersecting around the 4-fold axis. In view of the small number of unique reflections collected, we tried to find other solutions which captured the principal features of this 8(i) distortion with less new parameters added to the refinement. One such solution was found by allowing the Se(2) atoms to take on the form of two similar perpendicular cigar shaped ellipsoids, both centered on the 4-fold site, with anisotropic thermal parameters correlated to obey the symmetry of the site (even though individual ellipsoids break the symmetry). This solution is illustrated in Figure 1b. This increased the number of parameters from 11, for the solution with Se(2) at the 2(a) site, to 12 (for 173 unique reflections) and produced an  $R_w$  of 1.77%. This is statistically significant.<sup>9</sup> Final coordinates and thermal parameters for this solution are reported in Table Ia. Final occupation of the Se(2) site is at 84%. The 8(i) distortion is noteworthy as it does not correspond to the formation of  $\text{Se}_2^{2-}$  dimers between nearest selenium atoms as the 8(g) distortion does. It is of interest the Urland and Abriel<sup>4</sup> have reported an incommensurate lattice distortion in  $\text{PrSe}_{2.00}$  with a concomitant 8(g) distortion of the Se atoms.

(9) Hamilton, W. C. *Acta Crystallogr.* 1965, 18, 502.

(10) (a)  $\text{NdTe}_3$ : Norling, B. K.; Steinfink, H. *Inorg. Chem.* 1966, 5, 1488. (b)  $\text{Nd}_2\text{Te}_5$ : Pardo, M.-P.; Flahaut, J. *Bull. Soc. Chim. Fr.* 1967, 10, 3658.

Rb and Se(3). These values are within experimental error of an ideal value of  $\frac{1}{3}$  for both atoms. When all remaining occupancy factors were allowed to refine we found that none changed by more than 0.6%. Finally we removed the inversion center symmetry and refined the structure in  $Cmcm$ . There was no clearly significant drop in  $R_w$ . We therefore report this structure in the  $Cmcm$  space group.

Rubidium and selenium are respectively elements 37 and 34 of the periodic table. While these two elements have therefore similar diffracting power, they are chemically different. We assume that Rb and Se atoms will occupy crystallographically inequivalent sites. This assumption, coupled with the microprobe based stoichiometry, leads to the unique atomic assignment given in Table Ib. The atomic assignment of Table Ib has the virtue of leaving the structural sheet motifs known to occur in rare earth dichalcogenides and trichalcogenides intact. The Rb atoms are found to lie between sheets of Se atoms. This is strongly reminiscent of the position of alkali metal atoms in intercalated transition metal dichalcogenides.<sup>1k,l</sup> Bond distances for both  $\text{DySe}_{1.84}$  and  $\text{Rb}_{0.33}\text{DySe}_{2.67}$  are given in Table II.

## Discussion

Both  $\text{Rb}_{0.33}\text{DySe}_{2.67}$  and  $\text{DySe}_{1.84}$  can be related to the family of tetragonal and pseudotetragonal structure types which include the  $\text{NdTe}_3$ ,  $\text{Nd}_2\text{Te}_5$ , and  $\text{Cu}_2\text{Sb}$  (or  $\text{NdTe}_2$ ) structure types.<sup>3,10</sup> These structures all contain stackings of two different motifs.<sup>11</sup> The first motif is that of infinite square sheets of selenium atoms. The Se(2) atoms of  $\text{DySe}_{1.84}$  and the Se(2) and Se(3) atoms of  $\text{Rb}_{0.33}\text{DySe}_{2.67}$  form distorted versions of these square sheets, as is illustrated in Figures 1 and 2. Between these square sheets one finds a second structural motif which is composed of bilayers of rare-earth-metal atoms and  $\text{Se}^{2-}$  anions. These bilayers form a distorted net of face sharing cubes. In this second motif the rare-earth-metal atoms and the  $\text{Se}^{2-}$  atoms lie in an alternating arrangement such that each rare earth has five  $\text{Se}^{2-}$  neighbors and each  $\text{Se}^{2-}$  has five rare-earth neighbors. The Dy and Se(1) atoms of both  $\text{DySe}_{1.84}$  and  $\text{Rb}_{0.33}\text{DySe}_{2.67}$  form this second structural motif. Finally the  $\text{Rb}_{0.33}\text{DySe}_{2.67}$  structure contains a third structural motif, sheets of Rb atoms (as is illustrated in Figure 2). These structural motifs stack one upon another in this family of compounds. In the  $\text{DySe}_{1.84}$  structure, as in  $\text{Cu}_2\text{Sb}$ , one finds alternating layers of the Se square motif and the cubic Dy-Se motif, stacked along the  $c$  axis. In  $\text{Rb}_{0.33}\text{DySe}_{2.67}$  the order of the sequences is nearly the same but with half the cubic Dy-Se sheets replaced by layers of Rb atoms.

Of the various motifs found in these structures, the infinite square sheets are chemically the most interesting. Unlike atoms of the other structural motifs, the Se atoms do not have a completely filled electronic shell structure. In  $\text{DySe}_{1.84}$  the Se atoms of the square sheet have a partial charge of  $-1.2$  while for  $\text{Rb}_{0.33}\text{DySe}_{2.67}$  the average charge for atoms in the square sheet is  $-0.80$ . The Se  $p$ -band has therefore approximately 1 hole/square sheet Se atom. In the case of sulfur, the atom directly above selenium in the periodic table, this  $-1$  charge leads generally to the formation of  $\text{S}_2^{2-}$  dimers as is found in insulators such as marcasite, pyrite, and  $\text{LaS}_2$ .<sup>11</sup> By contrast, for tellurium

(11) See discussion in Pearson, W. B. *The Crystal Chemistry and Physics of Metals and Alloys*; Wiley: New York, 1972.

Table I. Atomic Positions and Thermal Parameters for  $DySe_{1.84}$  and  $Rb_{0.33}DySe_{2.67}$ 

atom	X/A	Y/B	Z/C	occupancy	$U_{11}$	$U_{22}$	$U_{33}$	$U_{23}$	$U_{13}$	$U_{12}$	$U_{eq}$
(a) $DySe_{1.84}$											
Dy	0.25	0.25	0.72729(8)	1.00	0.0106(2)	0.0106(2)	0.0253(3)	0.00	0.00	0.00	0.0155(1)
Se1	0.25	0.25	0.3681(1)	1.00	0.0087(3)	0.0087(3)	0.0163(6)	0.00	0.00	0.00	0.0112(2)
Se2	0.25	0.75	0.00	0.418(5)	0.125(4)	0.031(2)	0.0094(9)	0.00	0.00	0.00	0.055(1)
Se2'	0.25	0.75	0.00	0.418(5)	0.031(2)	0.125(4)	0.0094(9)	0.00	0.00	0.00	0.055(1)
(b) $Rb_{0.33}DySe_{2.67}$											
Dy	0.00	0.67906(2)	0.25	1.00	0.0093(2)	0.0127(2)	0.0073(2)	0.00	0.00	0.00	0.0098(1)
Rb	0.00	0.0153(1)	0.25	0.324(4)	0.024(2)	0.016(2)	0.052(3)	0.00	0.00	0.00	0.034(1)
Se1	0.00	0.79096(4)	0.25	1.00	0.0077(4)	0.0120(4)	0.0092(4)	0.00	0.00	0.00	0.0097(2)
Se2	0.00	0.40617(4)	0.25	1.00	0.0224(5)	0.0133(5)	0.0181(4)	0.00	0.00	0.00	0.0179(3)
Se3	0.00	0.09052(8)	0.1603(5)	0.328(2)	0.0153(9)	0.016(1)	0.020(1)	0.0068(7)	0.00	0.00	0.0169(6)

Table II. Bond Distances (Å) in  $DySe_{1.84}$  and  $Rb_{0.33}DySe_{2.67}$ 

(a) $DySe_{1.84}$	
Dy-1Se(1)	2.966(2)
Dy-4Se(1)	2.941(1)
Dy-4Se(2)	3.014(1)
Se(2)-4Se(2)	2.833(1) <sup>a</sup>
(b) $Rb_{0.33}DySe_{2.67}$	
Dy-Se(1)	2.962(2)
Dy-4Se(1)	2.921(1)
Dy-2Se(2)	2.979(2)
Dy-2Se(3)	3.120(2)
Rb-2Se(2)	3.531(3)
Rb-4Se(2)	3.495(3)
Rb-2Se(3)	3.225(4)/3.662(4) <sup>b</sup>
Se(3)-4Se(2)	2.583(1)/3.064(1) <sup>b</sup>

<sup>a</sup> In  $R_w = 1.66\%$  refinement with Se(2) in 8(i) position Se(2)-Se(2) distances distort to either 2.65(1) Å or 2.834(3) Å depending on the actual occupancy of the 8(i) positions. <sup>b</sup> Bond distances depend on which of the Se(3) sites are occupied.

and polonium, the elements directly beneath selenium in the periodic table, the presence of holes can lead to the formation of metallic structures. Such metallic structures are generally built up from cubes or square sheets Te or Po atoms.<sup>12</sup>

The square sheet of Se atoms found in  $DySe_{1.84}$  and  $Rb_{0.33}DySe_{2.67}$  appear to form as a compromise between the distorted insulating dimers found in the sulfides and the undistorted infinite square sheet metallic structures found for the heavier chalcogenides. The Se atoms in the square sheet lose their 4-fold symmetry as is indicated by the shape of the thermal ellipsoids of the Se(2) atom in  $DySe_{1.84}$  and the shift in position of the Se(3) atom in  $Rb_{0.33}DySe_{2.67}$ . In both systems the Se atoms, however, do not distort in the direction of the Se-Se bonds (as one might anticipate in the case of incipient  $Se_2^{2-}$  pair formation) but rather in a direction  $45^\circ$  away from any Se-Se bonds.

In both  $DySe_{1.84}$  and  $Rb_{0.33}DySe_{2.67}$  there is a clear nonstoichiometric character to the infinite square sheet motifs. In the case of the  $DySe_{1.84}$  subcell, there is only crystallographically equivalent site for the selenium atoms in these sheets with an overall occupation factor of 84%. In  $Rb_{0.33}DySe_{2.67}$  the square sheet has two crystallographically inequivalent sites: Se(2) is fully occupied, and Se(3) breaks the symmetry of the site and forms a pair of possible sites with an occupation factor of  $2/3$  for the pair ( $1/3$  each). Interestingly, the average overall occupation of selenium for both the square sheets in  $DySe_{1.84}$  and  $Rb_{0.33}DySe_{2.67}$  is  $5/6$  (within experimental error). For  $Rb_{0.33}DySe_{2.67}$  this fractional site occupancy variation creates a selenium site occupancy wave (SOW). The nearly equal site occupancy factors in  $DySe_{1.84}$  suggests that there may

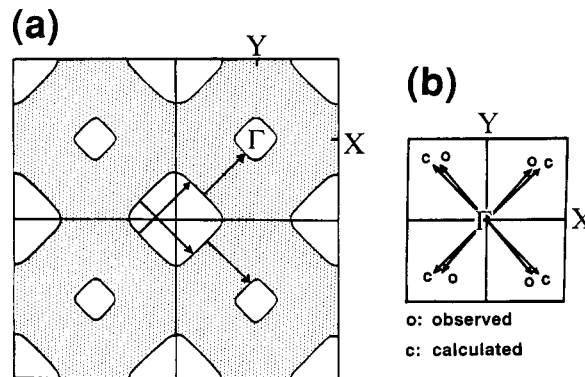


Figure 3. (a) Map of the extended Hückel Fermi surface in reciprocal space with nesting vectors. (b) Comparison of calculated nesting vectors with observed incommensurate wave vectors (projected onto the  $a^*b^*$  plane).

be a relation between the  $DySe_{1.84}$  and  $Rb_{0.33}DySe_{2.67}$  sheet structures. We expect, however, that the two sheet structures should differ in some manner due to their differing oxidation states. In particular, we suspect that the formation of  $Se_3^{4-}$ ,  $Se_5^{2-}$ ,  $Se_5^{4-}$ , and other higher polychalcogenide ions may be responsible both for the number of Se defects (the defects control oxidation state) and the Se atomic displacements. Such higher chalcogen polyanions are well-known.<sup>13</sup>

It is difficult to model the electronic structure of the partially occupied crystal lattices of such SOW materials. Nevertheless an extended Hückel<sup>14</sup> calculation of a fully occupied undistorted square sheet of  $Se^-$  atoms is of some interest. These calculations show that in the absence of any distortion of the square sheet the Se p-band is metallic. In Figure 3 we show a map of the Fermi surface in reciprocal space. As has been recently been shown by Whangbo and Canadell,<sup>15</sup> this extended Hückel calculation Fermi surface can be used to determine the possible CDW distortions. In particular, one must find vectors with maximal nesting, i.e., vectors which map as much of the Fermi surface onto itself as possible. Such vectors should correspond in principle to incommensurate lattice vectors. We show four

(13) (a)  $Te_5^{2-}$  (W-form): Teller, R. G.; Krause, L. J.; Haushalter, R. C. *Inorg. Chem.* 1963, 22, 1809. (b)  $Te_5^{4-}$  (Z-form): Böttcher, P.; Keller, R. *J. Less Comm. Met.* 1985, 109, 311. Bond angles in this paper for the Z-shaped  $Te_5^{4-}$  are  $105.3^\circ$  and  $180^\circ$ . These compare to bond angles of  $103.5(1)^\circ$  and  $180^\circ$  in the  $Rb_{0.33}DySe_{2.67}$  structure.

(14) (a) Hoffmann, R. *J. Chem. Phys.* 1963, 39, 1397. (b) Whangbo, M.-H.; Hoffmann, R. *J. Amer. Chem. Soc.* 1978, 100, 6093. (c) Discussion of square lattice structure is given in: Tremel, W.; Hoffmann, R. *J. Am. Chem. Soc.* 1987, 109, 124. This last work considers in detail the distortions of the square lattice to be found in GdPdS and CeAsS (d) extended Hückel parameters used were  $H_{ii}(4s) = -20.5$  eV,  $H_{ii}(4p) = -14.4$  eV,  $\zeta(4s) = 2.44$ ,  $\zeta(4p) = 2.07$  taken from: Hoffmann, R.; Shaik, S.; Scott, J. C.; Whangbo, M.-H.; Foshee, M. J. *J. Solid State Chem.* 1980, 34, 263.

(15) Whangbo, M.-H.; Canadell, E.; Foury, P.; Pouget, J.-P. *Science* 1991, 252, 96.

(12) Böttcher, P. *Angew. Chem.* 1988, 100, 781.

strong nesting vectors in Figure 3. Two vectors lie along the  $a^* + b^*$  direction, while the remaining two point along  $a^* - b^*$ . In Figure 4b we directly compare these vectors to the observed incommensurate wave vectors we find for  $\text{DySe}_{1.84}$ . It may be seen that the observed vectors are close in both magnitude and direction to the calculated ones. This agreement is somewhat surprising as the Whangbo-Canadell model is for CDW materials without site occupancy defects. These results are suggestive that the incommensurate diffraction observed in  $\text{DySe}_{1.84}$  is due to a charge density wave.

It is unfortunate that there is to date no theory which allows one to predict the occurrence of SOW in an analogous fashion. We are therefore not able to treat the exact issues raised by the  $\text{DySe}_{1.84}$  and  $\text{Rb}_{0.33}\text{DySe}_{2.67}$  sheet

structures as these materials contain SOWs in addition to any potential CDWs.

**Acknowledgment.** We would like to thank Dr. Jeff Kampf for recording the single-crystal X-ray data set and the donors of the Petroleum Research Fund, administered by the American Chemical Society, for financial support for this research. We would also like to thank Mr. Patrick O'Connell and Mr. Kenneth Ray, who prepared some of the reaction mixtures.

**Supplementary Material Available:** Tables of single-crystal collection and refinement data, Guinier powder pattern for  $\text{Rb}_{0.33}\text{DySe}_{2.67}$ , and Guinier powder pattern for  $\text{DySe}_{1.84}$  (4 pages); structure factor tables for  $\text{DySe}_{1.84}$  and  $\text{Rb}_{0.33}\text{DySe}_{2.67}$  (3 pages). Ordering information is given on any current masthead page.